Dalton Transactions

ROYAL SOCIETY OF CHEMISTRY

FRONTIER

View Article Online
View Journal | View Issue



Cite this: *Dalton Trans.*, 2026, **55**, 2799

# Beryllium gets going, finally. Recent highlights in the organometallic chemistry of beryllium

Bhagyashree Das and Vadapalli Chandrasekhar *

Beryllium, despite belonging to the s-block of the periodic table, has long remained a chemical enigma. Its notorious toxicity, stringent handling requirements, and limited availability have collectively stunted the pace of exploratory research compared to its heavier congeners. Yet, in the last decade, pioneering efforts by many research groups have challenged this narrative by uncovering a surprising spectrum of unusual and unprecedented molecular architectures of beryllium compounds. Recent advances have demonstrated that beryllium can engage in bonding and reactivity patterns previously considered inaccessible to s-block elements. These include the realization of multiple-bond character, the stabilization of low-coordinate and open-shell species, and the isolation of compounds featuring unusual electronic structures. Notable achievements encompass the synthesis of beryllium complexes supported by strong donor ligands such as CAACs, the isolation of diberyllocene featuring a Be–Be bond and the first structurally isolated beryllium radical cations and tricoordinate radical species. In parallel, the emergence of heterobimetallic systems featuring polarized Be–M interactions across the s-, p-, and d-blocks has underscored the ability of beryllium to engage in cooperative bonding and reactivity with diverse metal partners. This review aims to comprehensively document the recent breakthroughs in molecular organometallic chemistry of beryllium in the last decade, emphasizing the unusual bonding paradigms and reactivity that redefine the long-standing perception of s-block inertness.

Received 2nd December 2025,
Accepted 13th January 2026

DOI: 10.1039/d5dt02876k

rsc.li/dalton



## Introduction

The chemistry of beryllium has historically been relegated to the periphery of mainstream inorganic and organometallic chemistry research, largely due to the significant health hazards associated with exposure to beryllium and its compounds.[1–3] While the acute toxicity of $Be^{2+}$ ions is comparable to that of other commonly encountered toxic metal cations, such as $Ba^{2+}$, $Cd^{2+}$, $Hg^{2+}$, or $As^{3+}$, the primary risks associated with beryllium arise from its unique immunological response pathways following inhalation or dermal exposure. Consequently, experimental investigations involving beryllium require stringent exposure-control measures, including glovebox or HEPA-filtered containment, strict particulate-management protocols, and specialized training. As a result of these practical considerations, the molecular chemistry of beryllium has progressed more slowly than that of its heavier alkaline earth congeners, including magnesium, calcium, strontium, and barium. For decades, beryllium research was focused on niche applications such as ceramics, aerospace alloys, thin-film coatings, and nuclear materials science, with few contributions to molecular coordination or organometallic chemistry.[4–6]

Its combination of low density, high elastic modulus, and high melting point makes beryllium highly attractive for aerospace and space technologies.[6] In nuclear applications, beryllium's transparency to X-rays, low neutron capture cross-section, and strong neutron scattering render it indispensable as a plasma-facing material.[7] Beryllium oxide (BeO), with excellent thermal conductivity and radiation resistance, has been explored as an additive to uranium dioxide fuel pellets to improve heat dissipation.[8] In semiconductor science, beryllium is established as a reliable p-type dopant in GaAs and GaN.[9] Collectively, these applications underscore the dual nature of beryllium: a material of unparalleled promise, yet shadowed by its toxicity and the demanding safety protocols required for its industrial use.

Most alkaline earth metals (Mg, Ca, Sr, and Ba) exhibit bonding that is largely ionic, with weak orbital overlap and less directionality. Their larger size and low electronegativity make electrostatic interactions dominant. In contrast, beryllium, being the smallest and most electronegative of the alkaline-earth elements can form bonds with a high degree of covalency.[10] $Be^{2+}$ is the smallest ion among all the metal ions with an ionic radius of 0.59 Å which is smaller than that of $Li^{+}$ (0.60 Å), and an exceptionally high charge/radius ratio value of

*Tata Institute of Fundamental Research, Hyderabad-500046, India.*
*E-mail: vc@tifrh.res.in*

6.45 $Å^{-1}$,[11] far exceeding that of $Li^+$ (1.67 $Å^{-1}$).[12] Owing to these features, beryllium typically can engage in bonding with considerable covalent character. Furthermore, its small radius and high charge density can enforce strong orbital overlap with donor atoms (C, N, O), leading to short, directional, and polarized bonds. Thus, the chemistry of beryllium resembles p-block chemistry more than its s-block congeners. Like boron, beryllium is electron-deficient and often adopts unusual coordination geometries such as trigonal or linear arrangements. Be–X bonds display a strong degree of covalency and polarization like B–X bonds. Furthermore, the stabilization of Be(0) complexes (although the formal oxidation state in such complexes is contested) with CAAC ligands closely parallels the chemistry of carbene-stabilized Si(0), Ge(0), and Sn(0) species in group 14.[13–16] Likewise, the presence of Be–Be bonds in diberyllocene mirrors the bonding observed for B–B species[17] as well as heavier congeners such as Ga–Ga and Sn–Sn.[13,18,19] Taken together, these comparisons place beryllium in a conceptual bridge position between the ionic alkaline-earths and the covalent, electron-deficient p-block elements.

Nuclear magnetic resonance spectroscopy is a key tool for elucidating the bonding characteristics in molecular beryllium compounds. The only stable and naturally abundant isotope of beryllium, $^9$Be ($I$ = 3/2), is therefore the nucleus of choice for NMR investigations and provides a sensitive probe of the local electronic structure, coordination environment, and ligand donor properties.[20]

Despite a relatively slow start, the chemistry of beryllium is finally looking up. An excellent account by Kraus and Schulz has provided a comprehensive overview of modern molecular beryllium chemistry, while also clearly addressing the health hazards associated with beryllium and its compounds and outlining established protocols for their safe handling.[1] Buchner[2] has made significant contributions to elucidating the mechanisms associated with beryllium-related health risks and in promoting responsible experimental practices, which have been instrumental in enabling the continued development of the field. Together, these efforts have helped demystify beryllium chemistry and have laid a robust foundation for its safe and systematic exploration. Around this period and slightly afterwards, researchers have unveiled a series of unprecedented beryllium compounds that pushed the boundaries of main-group chemistry.[12,21–24] The discovery of s-block multiple bonding was first demonstrated through the isolation of di-*ortho*-beryllated carbodiphosphorane, offering direct evidence of a covalent Be=C linkage.[25] Perhaps, the most iconic advance was the report of diberyllocene, a genuine Be(I) species exhibiting a direct Be–Be bond.[12] The isolation of stable, crystalline beryllium radical cations further emphasized that open-shell electronic configurations could be accessed and stabilized in a controlled fashion.[21] Beyond these, unusual bonding motifs such as mono-*ortho*-beryllated carbodiphosphoranes and tricoordinate beryllium radicals have highlighted the versatility of beryllium in engaging with highly electron-rich or radical-stabilizing environments.[26,27] Importantly, cross-disciplinary insights emerged when a cyclic alkyl amino carbene bismuthinidene was isolated, mediated uniquely by a Be(0) complex, underscoring the role of Be fragments as reactive mediators in heavy main-group element chemistry.[28] The most recent developments, such as the formation of nucleophilic beryllyl complexes *via* metathesis at $[Be–Be]^{2+}$, reveal a surprising depth of Be–Be cooperation chemistry and nucleophilic reactivity in systems traditionally dominated by transition metals.[29] Parallel breakthroughs include the discovery of polarized heterobimetallic Be–M linkages spanning the s-, p-, and d-blocks, and the emergence of beryllium multiple bonding to carbon, nitrogen, and oxygen.[12,30–33] Other classes of beryllium compounds have been reported earlier, including dialkyls ($BeMe_2$, $BeEt_2$, $Be^tBu_2$), cyclopentadienyls ($BeCp_2$, $BeCp^*_2$), and halides/hydrides, which continue to serve as valuable precursors in film deposition and semiconductor doping.[1] Furthermore, the coordination and organometallic chemistry of beryllium has seen remarkable progress in the last decade. Classical aqueous motifs such as tetrahedral $[Be_3(\mu\text{-}OH)_3(donor)_6]^{3+}$ continue to dominate beryllium coordination chemistry; however, studies in non-aqueous media most notably liquid ammonia have significantly expanded the known speciation of $Be^{2+}$. In addition to simple ammine complexes such as $[Be(NH_3)_4]^{2+}$, systematic investigations have established the formation and structural characterization of tetra- and diammine beryllium halides and pseudohalides, as well as more complex amido- and oxyamidoberyllate species. These include tetra- and octanuclear amido clusters, unprecedented anionic amidoberyllates, and oxyamidoberyllate motifs formed *via* reactions of beryllium metal with ammonium or alkali metal reagents in liquid ammonia, highlighting the rich and previously underexplored coordination chemistry of beryllium in non-aqueous environments.[34]

Recent years have seen important progress in understanding Schlenk-type equilibria in organoberyllium chemistry, an area that underpins the structure, stability, and reactivity of Grignard-analogous Be reagents. In a detailed study, Buchner and co-workers[35] demonstrated that reactions of beryllium halides with diarylberyllium compounds in the presence of neutral donor ligands (N-, O-, C-donors) consistently favor heteroleptic species, rather than homoleptic analogues. Complementary work by Helling and Jones[36] systematically examined the role of aryl steric bulk in Schlenk-type redistribution processes of arylberyllium bromides. They showed that sterically demanding aryl groups suppress dynamic equilibria and stabilize discrete heteroleptic ArBeBr species, whereas less hindered systems engage in temperature-dependent equilibria or dimerization. These studies establish Schlenk equilibria as a central, yet controllable, feature of organoberyllium chemistry, analogous to classical Grignard reagents.

The use of modern ligands has opened new directions; NHCs enabled Be-induced carbene activation and the first structurally characterized beryllium borohydride $[\{(NHC)\}Be(BH_4)_2]$, scorpionate and amide complexes expanded bonding modes, and β-diketiminate systems uncovered unusual ether-cleavage and polymerization reactivity.[37,38] Organometallic

 

chemistry has likewise advanced, with the isolation of $BeMes_2$. ($Et_2O$), sterically hindered ArBeX complexes, and π-bound $BeCp^*_2$, and notably the first solid-state structure of a homoleptic berylliumorganyle, $BePh_2$, underscoring renewed progress in the structural characterization of fundamental beryllium–carbon bonding motifs.[39–41] Building on earlier reviews of beryllium chemistry,[1,42] this article highlights developments in the last decade, from 2016 to 2025, focusing on the unique, novel, and unusual bonding, reactivity, and electronic properties of organometallic compounds of beryllium that have emerged during this period (Fig. 1). Notably, the article highlights the isolation of beryllium compounds where beryllium is present in all three oxidation states (0, +1, and +2). This article also highlights the chemistry of beryllium which is based on its ability to form multiple bonds with other p-block elements. Together, these advances signal that beryllium chemistry is no longer confined to a few sentences in textbooks but is entering the major league opening new frontiers in s-block element science. A few selected examples that represent these advances are depicted in Chart 1.

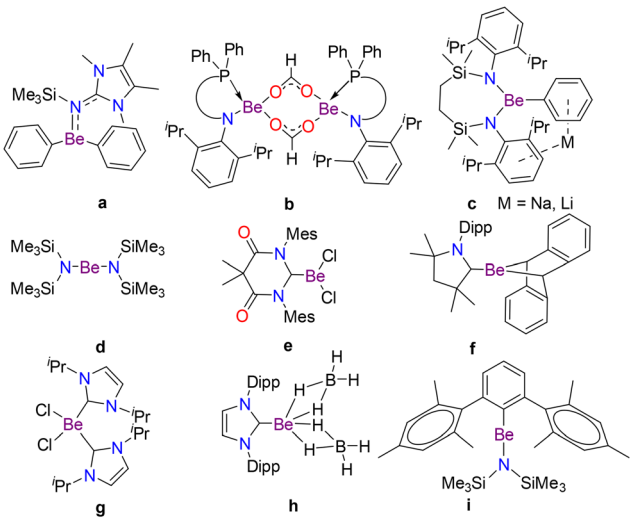


**Chart 1** Representative examples illustrating the diversity of organometallic beryllium complexes.[27,35,38,41,43,44–46]

## Bis(CAAC)-stabilized beryllium compounds

Low-valent main-group compounds are of considerable interest in main-group and organometallic chemistry due to the synthetic challenge, structure and reactivity.[49] Over the past decade, stable low-valent p-block compounds have emerged as valuable synthetic targets, displaying both transition-metal-like reactivity and unique bond-activation chemistry.[50] In contrast,[15,16,19,51,52] the chemistry of zero-valent s-block elements remains scarcely explored. Braunschweig *et al.* in 2016[23] reported the isolation of neutral Be(0) complexes stabilized by two cyclic (alkyl)(amino)carbene (CAAC) ligands, although the assignment of the zero oxidation state has been later challenged.[53–55]

The synthesis of the beryllium complexes **7** and **8** was achieved by reducing beryllium(II) species (**5** and **6**) in the presence of the **MeL**. The molecular structure of these compounds was confirmed by X-ray crystallography, which provided structural data consistent with a two-coordinate beryllium center, where the beryllium atom is bound to two CAAC ligands, forming a linear C–Be–C arrangement (C–Be–C bond angles are 180.00(7) and 179.3(2) for **7** and **8** respectively).

The Be–C bond lengths in **7** (1.664(2) and 1.659(5) Å) and **8** (1.659(4) and 1.657(4) Å) are significantly shorter than those

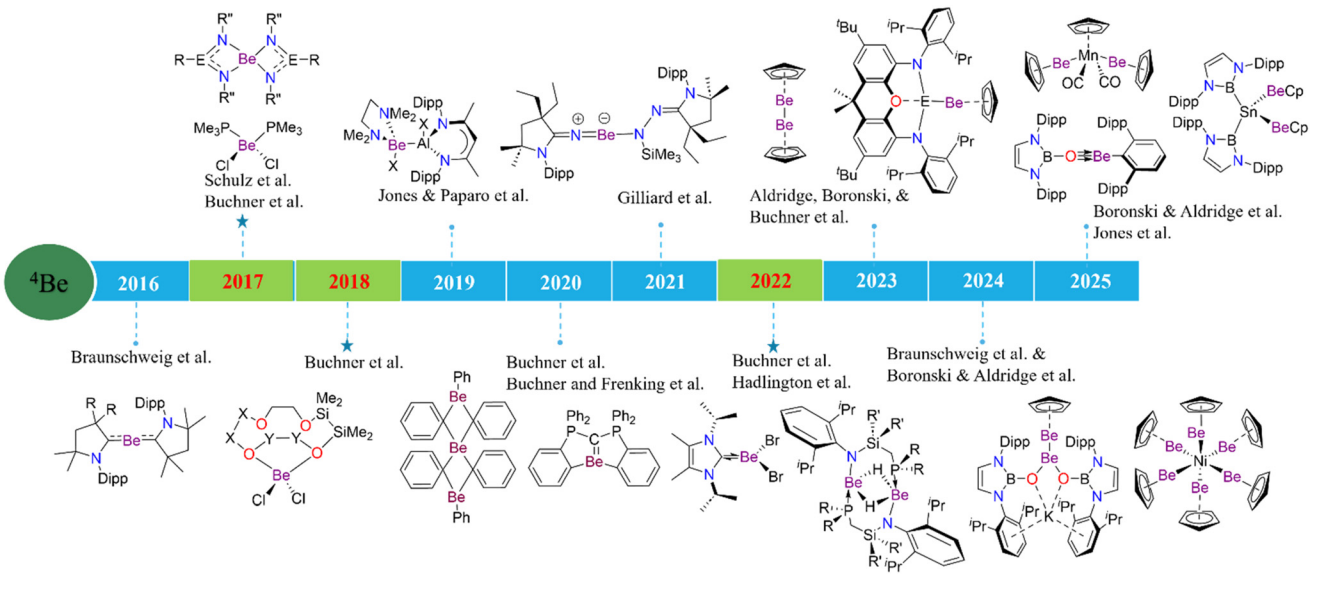


**Fig. 1** Chronological overview of beryllium chemistry in the last decade, depicting the progression of major discoveries, methodologies, and concepts. Dots indicate works discussed in this review, while stars denote works not covered.[12,12,22–25,27–33,40,46,47,48]

observed in compounds **5** (1.779(3) Å) and **6** (1.791(2) Å). The $^{9}$Be NMR resonance for these complexes appeared at ~32 ppm, which is downfield shifted compared to typical two-coordinate beryllium species[41,45] but still appearing upfield from other known complexes in the literature.[56] Interestingly, while **7** containing homoleptic ligands could be isolated from the reduction of **5**, an analogous reaction with **6** afforded the heteroleptic compound **8** (Scheme 1). The reaction of **7** with $CO_2$ and selenium, afforded the zwitterionic species **9** and selenone **10** (Scheme 1), respectively, with the removal of elemental beryllium, indicating the potential of these beryllium complexes to interact with small molecules.

The assignment of the formal oxidation state in the CAAC-supported beryllium complexes **7** and **8** has been the subject of active debate, as highlighted by several recent theoretical investigations.[53–55] In their analyses, Corral, Jana, Salvador, Andrada and coworkers[53] employed multireference methods, real-space bonding descriptors, and electron-density analyses to show that the Be–C interactions in these complexes are highly covalent, with substantial electron sharing between beryllium and the carbene ligands. On this basis, they argued that a classical oxidation-state description becomes ambiguous and that within a formal framework, the complexes may reasonably be described as Be(II) species supported by strongly donating CAAC ligands *i.e.*, $(L)^{-1}$–$(Be)^{2+}$–$(L)^{-1}$, rather than genuine low-valent beryllium compounds. In contrast, Pan and Frenking[54] analyzed the same systems using energy decomposition analysis, orbital interaction schemes, and charge-partitioning methods, and proposed that the electronic structure is best described as Be(0), with the CAAC ligands acting as neutral σ-donors and π-acceptors. There is no experimental evidence so far that demonstrates a chemical reactivity that unambiguously supports Be(0)-type behavior for these complexes. This absence of low-valent reactivity seems to support the Be(II)-based formulation advocated by Andrada and co-workers,[55] while simultaneously underscoring the limitations of assigning oxidation states in highly covalent main-group systems. Taken together, these studies demonstrate that the CAAC–beryllium complexes occupy a borderline electronic regime, where extreme covalency blurs the distinction between formal Be(0) and Be(II) descriptions.

Gilliard, Benkő, and coworkers[28] isolated a cyclic(alkyl)(amino)carbene–bismuthinidene complex using a Be-CAAC complex as a reducing agent. Starting from $(Et_2CAAC)Bi(Ph)Cl_2$ (**15**), attempts to reduce with $KC_8$ only led to decomposition and precipitation of Bi metal. The key breakthrough was the use of $Be(CAAC)_2$ (**13**), which acted both as a mild reducing agent and as a ligand-transfer reagent, thereby enabling the clean formation of the sub valent Bi(I) species (**14**) (Scheme 2).

## Be–M bonded (M = Be, B, Al, Ga, In, Sn, Fe, Ni, Mn and Re) molecules

Although low valent Mg(I)–Mg(I) and Ca(I)–Ca(I) dimers are well established,[57] analogous Be(I) complexes long remained elusive. In 2023, Aldridge, Boronski, and co-workers[12] synthesized diberyllocene (CpBe–BeCp) **18**, a stable Be(I)–Be(I) dimer, providing the first isolable Be–Be bond in molecular chemistry.

This was achieved through the reduction of $BeCp_2$ (**17**) with a dimeric magnesium(I) complex (**16**) (Scheme 3). Diberyllocene was fully characterized by X-ray crystallography, which confirmed a direct Be–Be interaction. The Be–Be bond length (2.0545(18) Å) in **18** is aligned with the sum of the single bond covalent radii for Be (2.04 Å).[58] The $^{9}$Be NMR spectroscopy of compound **18** shows a single high-field signal at −27.6 ppm, reflecting the electron-rich nature of the beryllium center. The ability of diberyllocene to act as a reducing agent forming beryllium–aluminyl compound (**19**) by treating **18** with (NON)AlI and a beryllium zinc compound (**20**) by treating

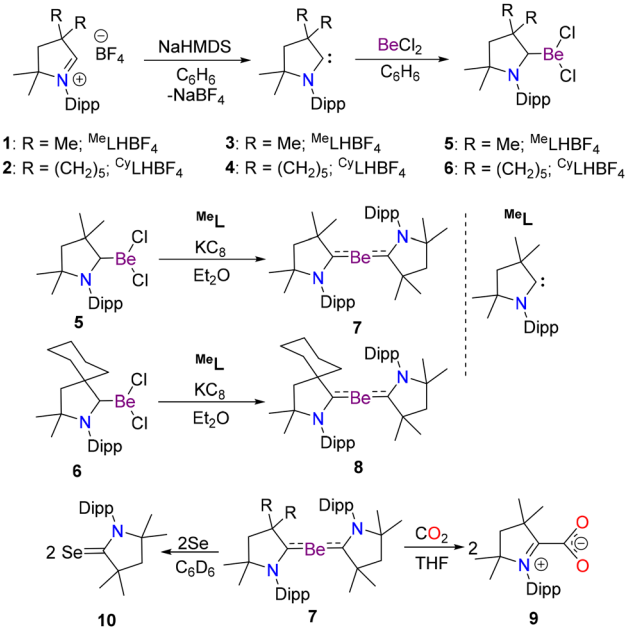


**Scheme 1** Synthesis of CAAC-stabilized beryllium(0) complexes **7** and **8**.[23]

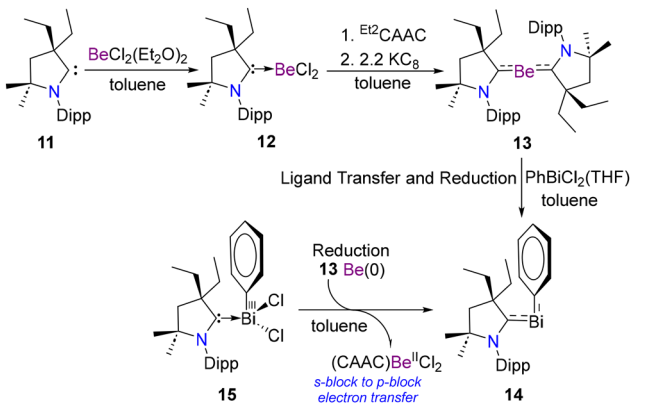


**Scheme 2** Synthesis of CAAC–bismuthinidene (**14**) by using **13** as a reductant and a ligand transfer agent.[28]

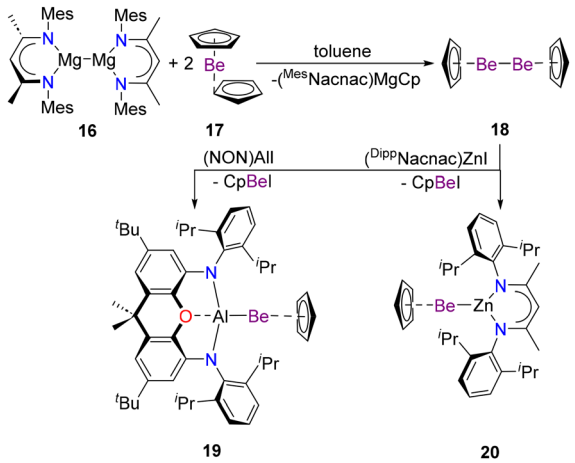


**Scheme 3** Synthesis and reactivity studies of the beryllium(I) compound (**18**).[12]

with ($^{Dipp}$Nacnac)ZnI, expanded the potential of organometallic beryllium compounds as reducing agents that could have synthetic applications (Scheme 3). The $^{9}$Be NMR chemical shift of **19** appears at −28.7 ppm. The diberyllocene **18** exhibits a comparable shift, indicating that its beryllium center is similarly electron-rich, consistent with a metal–metal bonded beryllium(I) species. Likewise, the Be–Zn complex shows a resonance at −27.7 ppm, which supports the presence of a highly electron-rich Be center, analogous to that in **18** and **19**.

Aldridge, Boronski, and co-workers in 2024[29] extended the chemistry of diberyllocene CpBe–BeCp (**18**) by demonstrating its ligand-metathesis reactivity (Scheme 4).

The reaction of **18** with KCp* gave Cp*Be–BeCp (**21**), while treatment with potassium boryloxide furnished the unsymmetrical complex [K{(HCDippN)$_2$BO}$_2$]Be–BeCp (**22**) (Scheme 4). X-ray diffraction confirmed intact Be–Be bonds, with **21** showing a bond length (≈2.05 Å) like **18**, whereas **22** displayed an elongated bond (≈2.135 Å), reflecting strong bond polarization. The $^{9}$Be NMR resonances were observed at −28.6 and −21.7 ppm for **21**, and −29.8 ppm (BeCp) and +9.5 ppm (BeNHBO) for **22** respectively, clearly evidencing the inequivalent electronic environments of the two Be centers. The Cp-bound Be thus appeared highly shielded, while the boryloxide-ligated Be was deshielded. Importantly, **22** acted as a source of the beryllyl anion [BeCp]$^-$, transferring it to electrophiles such as trityl cation [CPh$_3$]$^+$ to form a Be-carbon bonded compound (**24**) (Scheme 4). This reactivity mirrors that of sp$^2$–sp$^3$ diboranes,[59] underscoring unexpected parallels between beryllium and boron chemistry and establishing the first example of a polarized, mixed-valence Be$^0$/Be$^{2+}$ complex capable of nucleophilic Be transfer.

Harder, Buchner and co-workers reported in 2024[60] a heterobimetallic Mg–Be bonded complex, **26**, providing an example of a formal Be(0) species. The complex was synthesized in near-quantitative yield *via* salt-metathesis between **25** and the sterically accessible Cp*BeCl, whereas the more hindered Be[N(SiMe$_3$)$_2$]$_2$ was unreactive (Scheme 5). Single-crystal X-ray analysis revealed a nearly linear Mg–Be–Cp* motif in **26** with a Mg–Be distance of 2.469(4) Å, close to the sum of covalent radii, and elongated Be–Cp* contacts indicative of a low oxidation state at Be.

Multinuclear NMR spectroscopy showed retention of the solid-state structure in solution, with a markedly upfield $^{9}$Be resonance at *ca.* −23.7 ppm, signalling substantial electron density at Be. DFT calculations supported a strong yet polarized Mg–Be bond ($\Delta H_{homolytic} \approx 69.6$ kcal mol$^{-1}$), comparable to Be–Be bonding, with pronounced Mg$^{\delta+}$–Be$^{\delta-}$ character (NPA charges, Mg +1.21, Be +0.62). Despite this polarization, the complex is thermally robust and largely inert toward small

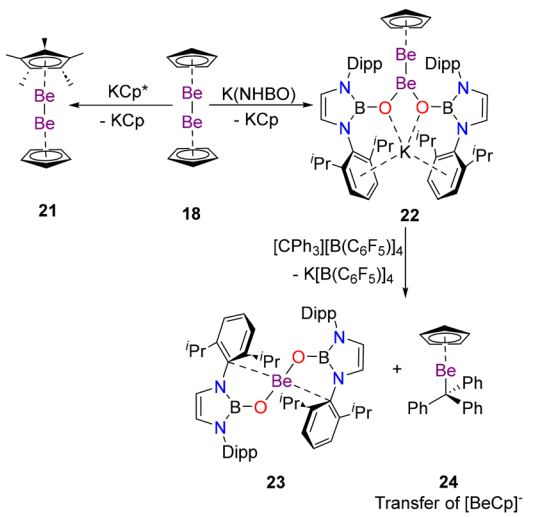


**Scheme 4** Synthesis of **21** and **22** through metathesis reactions with diberyllocene **18** and the reactivity of **22**.[29]

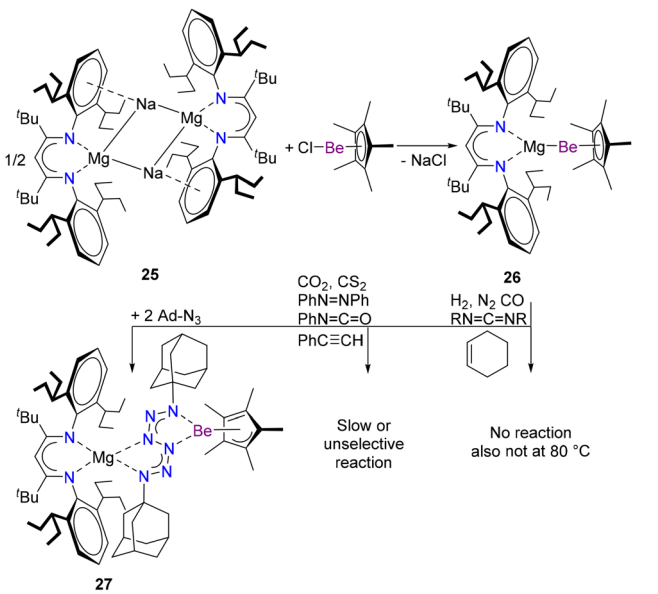


**Scheme 5** Synthesis and reactivity of Mg–Be compound **26**.[60]

molecules such as $H_2$, CO, and $N_2$, while reactions with benzophenone, azobenzene, phenylacetylene, $CO_2$, and $CS_2$ are slow and unselective. In contrast, reaction with 1-adamantyl azide leads to reductive coupling to form a $N_6$ chain **27**, accompanied by insertion of the azide into the Cp*–Be bond (Scheme 5).

Beyond direct Be–M bonding, unconventional beryllium–boron reactivity has further expanded this field. In a recent study, Buchner and co-workers[61] reported the first example of boron to beryllium transmetalation in phosphorus-based scorpionate systems, involving transfer of a $[CH_2P(^iPr)_2]^-$ fragment rather than a simple salt metathesis process. Even though compounds **28a** and **28b** do not contain a direct Be–B bond these are discussed in this section for the sake of continuity. Organo-beryllium complexes (**28**) are initially formed at low temperature, however the formation of **29** occurs *via* transmetalation, involving migration of the phosphanylmethyl unit from boron to beryllium (Scheme 6). Notably, Ph and $^n$Bu groups do not undergo transfer. This transformation constitutes the first experimentally verified transmetalation from a more electronegative element (B) to a less electronegative element (Be).

Jones *et al.* in 2019[48] reported the molecular complexes featuring covalent beryllium–aluminium (Be–Al) bonds. This work showed that beryllium, traditionally confined to halide or donor–acceptor chemistry, could in fact engage in unsupported, non-dative covalent bonding with another main-group element. By reacting beryllium dihalide adducts with an aluminium(I) heterocycle (**30**), the compound **31** was isolated, having a Be–Al bond (Scheme 7). DFT studies revealed a strong σ-character in the Be–Al bond and low polarity due to the nearly identical electronegativities of the two metals. The broader implication of this discovery is that beryllium can behave in a more transition-metal-like manner than previously recognized, with the capacity to form robust, covalent, and relatively nonpolar metal–metal bonds. Moreover, the Be–Al systems might have a potential utility as single-source precursors for Be–Al alloys, which have significant applications in aerospace materials.[62]

The reaction of beryllocene **17** with nucleophiles [K{E(NON)}] (**32**) (E = Al, Ga; NON = 4,5-bis(2,6-diisopropylanilido)-2,7-di-*tert*-butyl-9,9-dimethylxanthene) was reported by Aldridge, Buchner, and co-workers.[24] The substitution of one

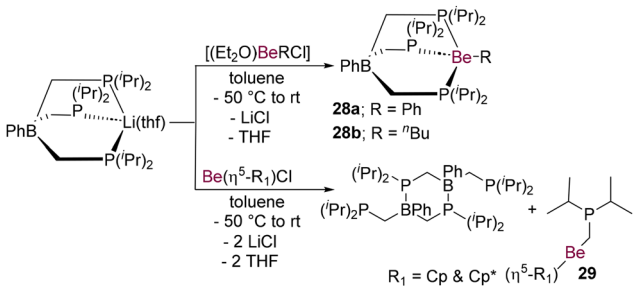


**Scheme 6** Synthesis of **28** and **29**.[61]

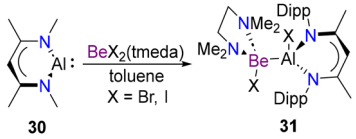


**Scheme 7** Synthesis of **31** which contains a Be–Al bond.[48]

Cp ligand in **22** leads to the formation of heterobimetallic complexes **19** and **33**, which contain direct Be–Al and Be–Ga linkages (Scheme 8). Remarkably, the Be–Al distance in **19** (2.310(4) Å) is shorter than in all previously reported analogues, and computational analyses identify a non-nuclear attractor (NNA) for the Be–Al bond, indicating that the electron density is concentrated between Be and Al rather than localised at the respective nuclei. Interestingly, because beryllium and aluminium have comparable electronegativities, the charge distribution is inverted relative to expectation; the Be atom (+1.39) is calculated to be less positively charged than Al (+1.88). Therefore, the Be center exhibits nucleophilic reactivity, a rare and counterintuitive behaviour for this element. Indeed, **19** and **33** react with *N*,*N*′-diisopropylcarbodiimide through nucleophilic attack at beryllium, affording a beryllium–diaminocarbene complex **34** and a guanidinate-type

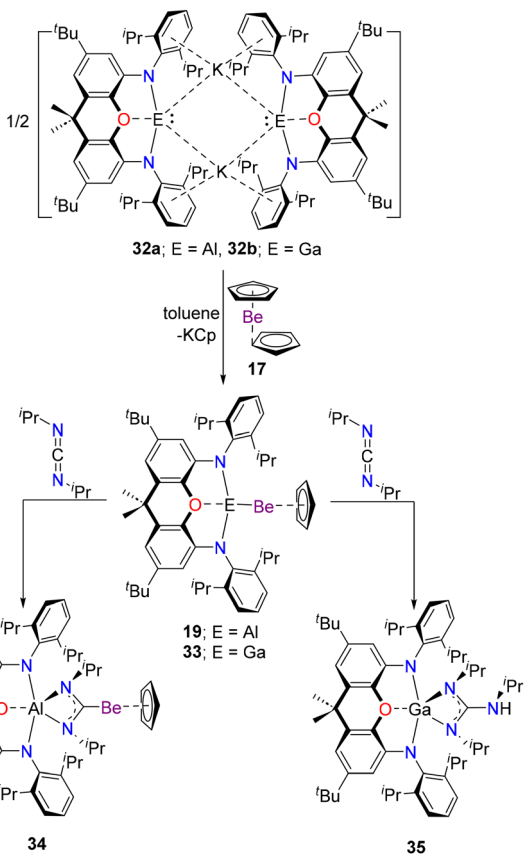


**Scheme 8** Synthesis and reactivity studies of Be–Al and Be–Ga compounds **19** and **33**.[24]

system coordinated to the gallium center **35**. However, in the case of the gallium–beryllium complex **33**, the observation is different, beryllium having a more positive charge than gallium. Consistently, the $^{9}$Be NMR resonances of **19**, **33** and nucleophilic addition product beryllium-diaminocarbene **34** appear at −28.7, −26.9, and −24.6 ppm, respectively.

Building on their earlier work on Be–Al (**19**) and Be–Ga (**33**) heterobimetallic systems, Boronski, Aldridge, and co-workers further expanded this chemistry in 2024[63] by isolating a Be–In molecular complex. Using an analogous salt-metathesis strategy to that employed for the aluminium and gallium congeners, reaction of $Cp_2Be$ with a nucleophilic indium(I) precursor [(NON)In]K enabled selective substitution of a Cp ligand and formation of **36** (Scheme 9).

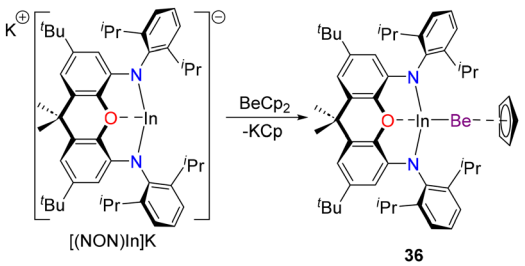


**Scheme 9** Synthesis In–Be compound **36**.[63]

In 2025, the scope of Be–E bonding was expanded to group 14 with the isolation of the first structurally Sn–Be molecular complex reported by Dietz, Boronski, Aldridge and co-workers.[32] In this study, a bis(boryl)stannylene, **37** was found to undergo a formal reductive addition of a Be–Be bond upon reaction with **18**, affording the heterometallic complex **38** (Scheme 10) containing the first structurally confirmed Sn–Be bond. Single-crystal X-ray analysis revealed a tetrahedral tin centre bearing two boryl and two beryllyl ligands. The Sn–Be bond lengths (2.388(3) and 2.389(3) Å) are slightly shorter than the sum of the covalent radii, while the long Be···Be separation (3.577(6) Å) confirms complete cleavage of the Be–Be bond. Based on electronegativity considerations, this process is best described as reductive addition of Be–Be bond at Sn(II), leading to a formal Sn(0) assignment.

Multinuclear NMR spectroscopy further supports the solid-state structure. The $^{9}$Be NMR spectrum of **38** displays a single resonance at −24.5 ppm, accompanied by unresolved $^{117/119}$Sn satellites, providing direct spectroscopic evidence for Sn–Be bonding. Due to coupling with multiple quadrupolar nuclei, no resolved $^{119}$Sn NMR resonance was observed for this complex.

A significant expansion of beryllium chemistry into the d-block has been realized through the isolation of well-defined iron– and nickel–beryllyl complexes by Boronski, Aldridge, and coworkers in 2024,[30] demonstrating that controlled Be–Be bond activation provides access to unprecedented heterometallic bonding motifs. Reaction of 0.5 equivalents of $Fe_2(CO)_9$ with **18** furnished the diamagnetic 18-electron complex **39** (Scheme 11). Single-crystal X-ray diffraction establishes a *cis*-octahedral coordination geometry at iron, with short Fe–Be distance in **39**. The corresponding $^{9}$Be NMR spectrum of **39** displays a single resonance at $\delta(^{9}\mathrm{Be}) \approx -18.0$ ppm, substantially downfield relative to **18** ($\delta \approx -27.6$ ppm), supporting the absence of Be–Be bonding and highlighting enhanced Be → Fe σ donation in the heterobimetallic framework.

An even more striking manifestation of beryllyl donor strength is observed in the nickel system. Treatment of Ni(COD)$_2$ with three equivalents of **18** leads cleanly to Ni(BeCp)$_6$ (**40**) (Scheme 11). X-ray crystallographic analysis reveals a highly symmetric pseudo-octahedral environment at nickel, defined exclusively by six BeCp ligands, with exceptionally short Ni–Be bond lengths that underscore the strong covalent character of the interaction. The electronic structure of this complex is highly unusual: population of nickel 4p-based orbitals gives rise to an inverted ligand field, while multicenter NiBe$_6$ bonding interactions contribute to the stabilization of the formally high-valent coordination environment. The $^{9}$Be NMR spectrum of **40** consists of a single resonance at $\delta(^{9}\mathrm{Be}) = -16.7$ ppm, the most downfield shift reported for any CpBeX-type complex. This pronounced deshielding has been attributed to strong metal–beryllium orbital mixing and possible aromatic ring-current effects within the delocalized NiBe$_6$ framework, and contrasts sharply with the high-field shift observed for Be–Be bonded species such as **18**. Collectively, these studies establish beryllyl ligands as uniquely potent donors capable of stabilizing highly unusual coordination numbers and electronic structures at transition metals.

Additionally, Boronski, Aldridge, and co-workers[31] reported the synthesis of bis(beryllyl) manganese and rhenium complexes as reactive intermediates for hydrocarbon beryllation. Photolysis of CpMn(CO)$_3$ or CpRe(CO)$_3$ with **18** in cyclohexane at ambient temperature affords *trans*-CpMn(CO)$_2$(BeCp)$_2$ (**42**) and *trans*-CpRe(CO)$_2$(BeCp)$_2$ (**41**), respectively (Scheme 12). Both complexes are diamagnetic 18-electron species adopting

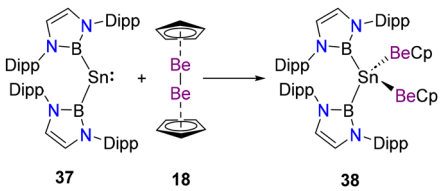


**Scheme 10** Synthesis of Sn(0) complex **38** from stannylene **37**.[32]

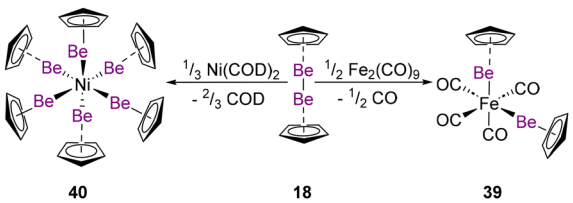


**Scheme 11** Synthesis of Be coordinated Fe **39** and Ni **40** complexes.[30]

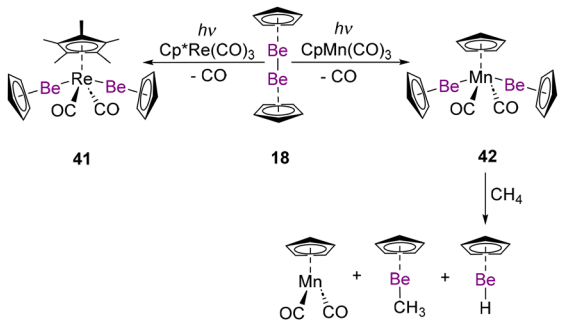


**Scheme 12** Synthesis of Be–Re (**41**) and Be–Mn (**42**) complexes and the reactivity of **42**.[31]

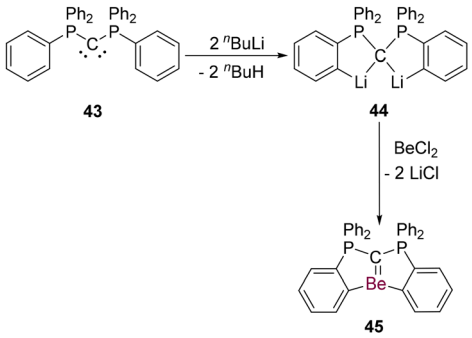


**Scheme 13** Synthesis of **45** by using carbodiphosphorane ligand **43**.[25]

a four-legged piano-stool geometry with trans-oriented BeCp ligands. Single-crystal X-ray analysis showed Mn–Be distances of 2.169–2.172 Å and Re–Be distances of 2.298–2.316 Å in **42** and **41** respectively. The $^{9}$Be NMR spectra exhibit resonances at −12.5 ppm (**42**) and −10.5 ppm (**41**), indicating the electron-rich and Lewis acidic nature of the beryllium centers. Notably, both complexes react with methane under ambient photochemical conditions to produce CpBeMe and CpBeH, demonstrating the unique ability of beryllyl ligands to mediate C–H elementation that is inaccessible to analogous boryl systems.

### Be–E (E = C, N and O) multiple bonded compounds

The multiple bond chemistry of main-group elements[64] is uncommon for s-block metals owing to the predominantly ionic bonding character of these metals. Nevertheless, recent years have witnessed a series of seminal discoveries demonstrating that beryllium can engage in multiple bonding with carbon, nitrogen, and oxygen, thereby redefining the bonding capabilities of s-block.

A landmark breakthrough in this context was reported by Buchner, Frenking, Sundermeyer and co-workers[25] with the synthesis of a di-*ortho*-beryllated carbodiphosphorane featuring a Be=C, representing the first experimentally example of a metal–carbon double bond involving an s-block element. **45** was accessed *via* a salt elimination strategy using a carbodiphosphorane ligand bearing *ortho*-functionalized aryl substitutents **43**, where deprotonation generated a dianionic precursor **44** that reacted with a beryllium halide under inert conditions to afford an air- and moisture-sensitive crystalline material (Scheme 13).

Single-crystal X-ray diffraction revealed a markedly shortened Be–C bond distance 1.704(2) Å in **45** relatives to typical Be–C single bonds of Be-CDP and Be-CDC and a near-coplanar Be–C–P arrangement, enabling effective π-donation from the carbodiphosphorane carbon lone pair into the vacant Be 2p orbital. Complementary DFT calculations, together with EDA-NOCV analyses, established that the Be=C interaction consists of a dominant σ-donation accompanied by a substantial π-donation component, providing compelling evidence for multiple-bond character.

Early experimental evidence for Be=N multiple bonding was provided by Schulz and co-workers in 2015,[45] who reported the first solid-state structure of the monomeric beryllium diamide Be[N(SiMe$_3$)$_2$]$_2$ and demonstrated, through combined X-ray diffraction and DFT analyses, that the Be–N interaction is predominantly ionic but exhibits a significant partial Be=N double-bond character. Building on this conceptual advance, Gilliard, Wilson, and co-workers[22] reported the first isolable beryllium imido complex Be=NR (**46**) in 2021, marking a significant extension of multiple-bond chemistry to Be–N systems. **46** was obtained by the oxidation of **13** with trimethylsilyl azide (Scheme 14).

The molecular structure revealed a remarkably short Be–N bond length of 1.464 Å. The $^{9}$Be resonance at 9.01 ppm is notably upfield shifted. DFT studies supported the existence of a strong π-interaction between beryllium and nitrogen, arising from overlap of the Be 2p orbitals with the N lone pair (**46b**). NBO and energy decomposition analyses reinforced the view that the Be=N bond approaches a true double bond in **46a**, albeit with some polarity toward nitrogen.

Buchner *et al.*[44] subsequently expanded the Be–N bonding landscape by synthesizing imide complex [Be(NCPh$_2$)$_2$]$_3$ (**47**), prepared *via* protonolysis of Be($^{i}$Bu)$_2$ with diphenylmethanimine (HNCPh$_2$) under thermal conditions (Scheme 15). Single-crystal X-ray diffraction revealed short Be–N bonds to the terminal imido nitrogen atoms 1.502(3) and 1.507(3) Å compared to the bridging nitrogen atoms. Detailed Computational studies demonstrated that the Be–N bonds comprise covalent σ inter-

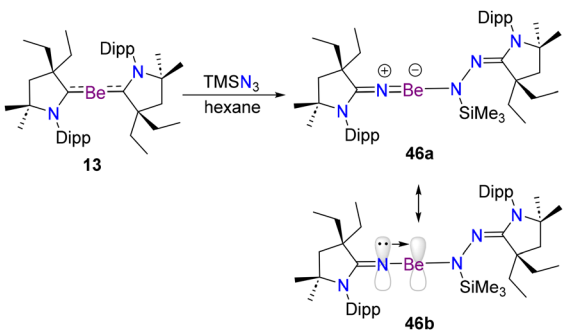


**Scheme 14** Synthesis of beryllium(II) imido complex (**31**).[22]

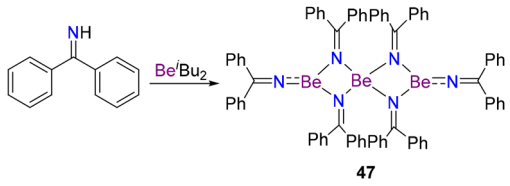


**Scheme 15** Synthesis of **47**.[44]

actions supplemented by significant π-donation from nitrogen lone pairs, resulting in partial Be═N double-bond character that is distributed over multi-centre bonding motifs rather than localized at a single Be–N unit.

Zhou *et al.*[65] identified transient HNBeCO with computational evidence for Be–N triple bonding. Also, Be–O and Be–F multiple bonds had been predicted computationally.[66,67]

These computational predictions were realized experimentally in 2025 by Jones *et al.*,[33] who synthesized monomeric two-coordinate beryllium complexes featuring Be–N and Be–O triple bonds. **48** and **49** were synthesized by reacting Be(II) precursors with appropriate ligands, stabilizing highly covalent

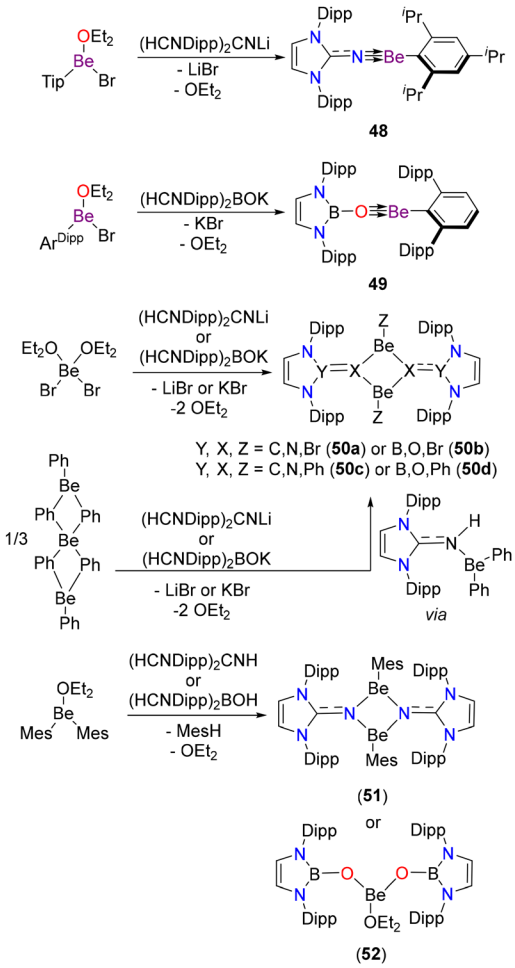


**Scheme 16** Isolation of Be–N and Be–O triple-bonded compounds **48**, **49** and dimeric compounds **50**, **51**.[33]

Be–N and Be–O triple bonds (Scheme 16). This work demonstrated that beryllium could form stable, low-oxidation-state multiple bonds with both nitrogen and oxygen. Notably, the $^9$Be NMR resonances for **48**, and **49** appeared at 12.3 and 11.0 ppm, respectively indicating the highly deshielding, covalent environments of beryllium in these compounds. The X-ray crystallography of these complexes revealed strong Be–N (1.434(2) Å, 1.437(3) Å) and Be–O (1.4035(14) Å) bonds, which were further confirmed by computational studies. However, smaller aryl substituents (Ph, Mes) afforded dimeric structures (**50** and **51**) (Scheme 16).

A more explicit cross-comparison of Be–E bonding analyses highlights that beryllium engages in markedly different bonding regimes depending on the electronegativity and orbital compatibility of the partner element. In Be–N and Be–O multiple-bonded systems, such as terminal imido Be═NR[22] in **46** and oxo-like Be≡O[33] in **49** species, the Be–N (1.46 Å) and Be–O (1.40 Å) distances are significantly shorter than typical Be–X single bonds (>1.70 Å), and indicative of substantial π character, noting that beryllium intrinsically forms short bonds to electronegative elements due to its small size and high polarizing power. Computational analyses (NBO, EDA-NOCV, QTAIM) consistently show strong but highly polarized π- interactions, where the π-electron density resides predominantly on the electronegative N or O atoms, supporting a formal Be(II) description despite the presence of multiple-bond features.

### Beryllium radical and radical cation species

The isolation and stabilization of main group radical cations is inherently challenging. While, examples of stabilization of p-block radical cations are now well established,[68] the stabilization of s-block radical cations remains significantly more difficult. In 2020, however, Gilliard *et al.*[21] reported a breakthrough in this area with the isolation of the beryllium radical cation, $[(CAAC)_2Be]^{\bullet+}$ (**53**) (Scheme 17), thereby opening the door to open-shell beryllium chemistry. A one-electron oxidation of **13** using TEMPO afforded a radical cation, **53**, whose EPR spectrum indicated substantial delocalization of the unpaired electron over the NCBeCN framework. Consistent with this description, spin-density analysis revealed only partial localization at the beryllium center (0.38 e Å$^{-3}$), with significant contributions from the carbene carbon atoms (0.18 e Å$^{-3}$ each) and the nitrogen atoms (0.13 e Å$^{-3}$ each). Hyperfine coupling to $^9$Be further confirmed Be participation in the singly occupied molecular orbital. Treatment of **53** with $NaBArF_4$ afforded **54** and the trimetallic disodium/beryllium cation (**55**). **53** could be reduced with $KC_8$ to regenerate **13**, along with a bimetallic K/Be species (**56**) (Scheme 17).

In 2024, Braunschweig *et al.* advanced the beryllium radical chemistry by isolating an open-shell tricoordinate Be compound, [(CAAC)(Et$_2$O)BeDur]·(2-Et$_2$O) (**58**), synthesized through the one-electron reduction of a CAAC–Be precursor (**57**) (Scheme 18).[27] DFT spin-density analysis and EPR calculations revealed that only a small fraction of the unpaired spin density (3 to 6%) is localized at the beryllium center, with the majority delocalized over the CAAC carbon (57–72%) and the nitrogen

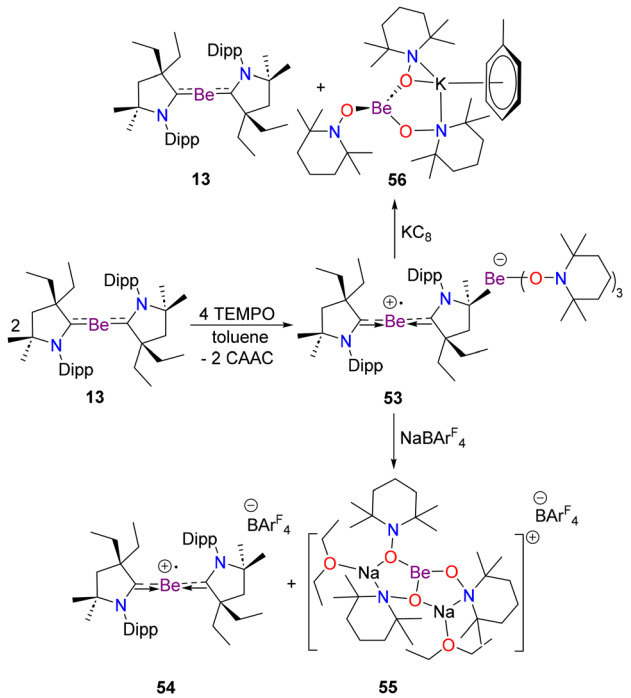


**Scheme 17** Isolation and reactivity study of beryllium radical cation (**53**).[21]

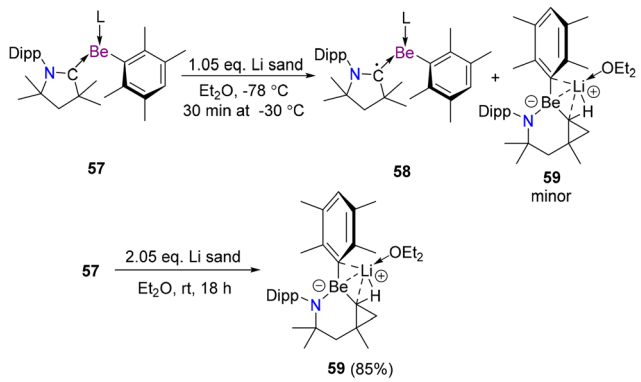


**Scheme 18** Synthesis of tricooordinated beryllium radical **58** and beryllacycle **59**.[27]

center (16–19%). These findings support a bonding description in which **58** is best regarded as a formal Be(II) complex bearing a reduced $[CAAC]^{\bullet-}$ ligand rather than a true Be(I) species. These stable radicals exhibited ligand exchange and C–H activation reactions, which resulted in a beryllacycle (**59**) as a minor product when 1.05 equiv. of lithium sand was used. However, **59** could be isolated in 85% yield by using 2.05 equiv. of lithium sand.

**$^9$Be NMR spectroscopy as a probe of electronic structure.** $^9$Be NMR spectroscopy provides valuable qualitative insight into the electronic structure, oxidation state, and coordination environment of molecular beryllium species. Highly deshielded resonances at strongly positive chemical shifts ($\delta \approx$ +25 to +32 ppm) are characteristic of low-coordinate, electron-rich beryllium centers, particularly zero-valent or strongly σ-donating carbene-stabilized Be species (Table 1).

For example, bis(CAAC)-stabilized Be(0) complexes exhibit the most downfield shifts observed to date ($\delta \approx$ +32 ppm), reflecting significant electron density at Be combined with minimal coordination (Table 1). In contrast, classical two-coordinate Be(II) complexes supported by strong σ-donor ligands such as CAACs, imido, nitrido, or oxo ligands cluster in a narrower range between +9 and +14 ppm. This consistency suggests that for low-coordinate Be(II) species, the $^9$Be chemical shift is governed primarily by coordination number rather than the identity of the terminal multiple-bonded ligand.

A marked upfield shift (negative $\delta$ values) is observed upon formation of Be–Be or Be–metal bonds. Be(I)–Be(I) dimers, Cp*-supported Be–Be systems, and heterobimetallic complexes with Al, Ga, Zn, Sn, Mg, and transition metals typically resonate between −10 and −30 ppm (Table 1). This pronounced shielding is consistent with increased covalency, metal–metal bonding interactions, and effective electron delocalization away from the Be center. Mixed-valence systems display two distinct resonances, directly reflecting inequivalent Be oxidation states within the same molecule. Overall, the available $^9$Be NMR data demonstrate that chemical shifts become progressively more shielded with increasing coordination number, metal–metal bonding, and covalent character.

**Table 1** $^9$Be NMR chemical shift values for representative beryllium complexes

| $^9$Be $\delta$ (ppm) | Compounds | Description |
|---|---|---|
| +32.0 | **7** & **8** | Bis(CAAC)-stabilized Be(0) complexes |
| +26.3 | **45** | Be=C bonded molecule |
| +13.7 | **12** | CAAC-stabilized Be(II) complex |
| +12.9, +12.8 | **5** & **6** | CAAC-stabilized Be(II) complexes |
| +12.3 | **48** | Monomeric two-coordinate Be≡N (nitrido-type) species |
| +11.0 | **49** | Monomeric two-coordinate Be≡O (oxo-type) species |
| +10.6 | **54** & **55** | Radical cationic Be species and trimetallic disodium–beryllium cation |
| +9.5 | **22** | Mixed-valence Cp–Be–Be–boryloxide (Be (II) site) |
| +9.0 | **46** | Terminal Be(II) imido complex (Be=NR) |
| +7.52 | **56** | Bimetallic potassium–beryllium complex |
| −10.5 | **41** | Be–Re heterobimetallic complex |
| −12.5 | **42** | Be–Mn heterobimetallic complex |
| −16.7 | **40** | Be–Ni heterobimetallic complex |
| −18.0 | **39** | Be–Fe heterobimetallic complex |
| −21.7 | **21** | Cp*Be–BeCp (Be–Be bonded site) |
| −23.7 | **26** | Cp*Be fragment in Mg–Be complex |
| −24.5 | **38** | Be–Sn heterobimetallic complex |
| −24.6 | **34** | Low-coordinate beryllium diaminocarbene complex |
| −26.9 | **33** | Be–Ga heterobimetallic complex |
| −27.6 | **18** | Be(I)–Be(I) bonded dimer |
| −27.7 | **20** | Be–Zn heterobimetallic complex |
| −28.6 | **21** | Cp*Be–BeCp |
| −28.7 | **19** | Be–Al heterobimetallic complex |
| −29.8 | **22** | Mixed-valence Cp–Be–Be–boryloxide (Be (I) site) |
| — | **31** | Be–Al complex ($^9$Be resonance not observed due to quadrupolar broadening) |

## Conclusions

Although beryllium chemistry remains one of the least explored areas in the periodic table due to the toxicity and challenging handling requirements of this element, as well as its low availability, the last decade has produced a series of remarkable discoveries that have redefined its chemical profile. In this review, we specifically focused on the recently developed novel and unusual properties of beryllium, which showcase its ability to transcend the boundaries traditionally associated with s-block chemistry. The pioneering work on CAAC-stabilized Be complexes opened the door to concepts once thought unattainable for an s-block element, such strong π-backbonding, multiple bonding, and radical stabilization. Subsequent studies have demonstrated that beryllium could engage in covalent metal–metal bonding, sustained radical and open-shell species, and even form multiply bonded Be═C, Be═NR and Be≡X (N, O) units with unprecedented bond strengths and reactivity patterns. These advances establish beryllium as an outlier within the alkaline-earth series, displaying transition-metal-like features despite belonging to the s-block. Taken together, these findings underline that beryllium is not merely a lightweight, toxic, and industrially relevant metal but also a unique element capable of supporting bonding motifs and reactivity modes previously reserved for the p- and d-blocks. By stabilizing unusual oxidation states (0, +1, and +2), enabling radical reactivity, and forming strong covalent and multiple bonds (double and triple bonds), beryllium has emerged as a fertile ground for conceptual advances in main-group chemistry. It must be mentioned that the nature of bonding including the formal oxidation states of beryllium in these compounds would be subject to more intense theoretical studies and will remain a subject of debate.[53–55,67] While experimental exploration will remain limited by safety concerns, the discoveries highlighted here underscore that beryllium can no longer be regarded as an outlier but rather as a versatile element with potential to inspire new directions in bonding, reactivity, and materials design. Looking ahead, the field of beryllium chemistry offers several compelling directions that extend far beyond the discoveries reported to date. One of the most immediate needs is a deeper theoretical understanding of the unusual bonding scenarios now known for Be, particularly in species exhibiting strong π-back bonding, multiple bonding and the typical oxidation states such as Be(0) and Be(I). At the same time, the design of ligand frameworks especially those combining strong σ-donation with controlled π-acceptor ability, or incorporating redox-active or multidentate architectures can hold promise for stabilizing even more reactive or unconventional beryllium species. Further exploration of metal–metal interactions, including heterometallic Be-transition and rare earth metal systems may reveal cooperative reactivity or new modes of small molecule activation. In particular, the emerging radical and open-shell chemistry of beryllium points to exciting possibilities in activating $H_2$, $CO_2$, $N_2O$, and unsaturated substrates, potentially through mechanistic pathways distinct from both s- and p-block analogues. Finally, progress in experimental strategies, and the development of bench-stable beryllium transfer reagents will be crucial to expanding the accessible chemical space.

## Author contributions

B. D. prepared the draft based on suggestions from V. C.; V. C.: project administration, supervision, reviewing, and editing.

## Conflicts of interest

There are no conflicts to declare.

## Data availability

This review article provides a summary of recent advances in organometallic beryllium chemistry. All schemes, and the characterization data discussed are derived from previously published literatures, which are cited in the references. No original experimental data were produced in this work.

## Acknowledgements

V. C. is thankful to the Dept of Science and Technology, New Delhi, India, for a National J. C. Bose Fellowship. B. D. is grateful to the Tata Institute of Fundamental Research, Hyderabad, for a postdoctoral fellowship.

## References

1 D. Naglav, M. R. Buchner, G. Bendt, F. Kraus and S. Schulz, *Angew. Chem.*, 2016, **128**, 10718–10733.
2 M. R. Buchner and M. Müller, *ACS Chem. Health Saf.*, 2023, **30**, 36–43.
3 M. R. Buchner, *Z. Naturforsch., B:J. Chem. Sci.*, 2020, **75**, 405–412.
4 (*a*) A. R. Berry and C. W. Nordin, *Thin Solid Films*, 1992, **217**, 83–86; (*b*) B. J. Mulder, *Thin Solid Films*, 1978, **55**, 35–40.
5 *Beryllium chemistry and processing*, ed. K. A. Walsh, ASM International, Materials Park OH, 2009.
6 R. Puchta, *Nat. Chem.*, 2011, **3**, 416.
7 M. Merola, D. Loesser, A. Martin, P. Chappuis, R. Mitteau, V. Komarov, R. A. Pitts, S. Gicquel, V. Barabash, L. Giancarli, J. Palmer, M. Nakahira, A. Loarte, D. Campbell, R. Eaton, A. Kukushkin, M. Sugihara, F. Zhang, C. S. Kim, R. Raffray, L. Ferrand, D. Yao, S. Sadakov, A. Furmanek, V. Rozov, T. Hirai, F. Escourbiac, T. Jokinen, B. Calcagno and S. Mori, *Fusion Eng. Des.*, 2010, **85**, 2312–2322.

8 (*a*) S. Ishimoto, M. Hirai, K. Ito and Y. Korei, *J. Nucl. Sci. Technol.*, 1996, **33**, 134–140; (*b*) R. Latta, S. T. Revankar and A. A. Solomon, *Heat Transfer Eng.*, 2008, **29**, 357–365; (*c*) W. Zhou, R. Liu and S. T. Revankar, *Ann. Nucl. Energy*, 2015, **81**, 240–248.
9 (*a*) J. D. Parsons, L. S. Lichtmann, F. G. Krajenbrink and D. W. Brown, *J. Cryst. Growth*, 1986, **77**, 32–36; (*b*) T. Kobayashi, K. Kurishima and T. Ishibashi, *J. Cryst. Growth*, 1994, **142**, 1–4.
10 L. P. Griffin and J. T. Boronski, *Dalton Trans.*, 2025, **54**, 13020–13029.
11 J. T. Boronski, *Dalton Trans.*, 2023, **53**, 33–39.
12 J. T. Boronski, A. E. Crumpton, L. L. Wales and S. Aldridge, *Science*, 2023, **380**, 1147–1149.
13 R. K. Siwatch, Z. J. G. Ng, J.-J. S. Lim, Z.-F. Zhang, M.-D. Su and C.-W. So, *J. Am. Chem. Soc.*, 2025, **147**, 20251–20256.
14 K. Chan, F. Ying, D. He, L. Yang, Y. Zhao, J. Xie, J.-H. Su, B. Wu and X.-J. Yang, *J. Am. Chem. Soc.*, 2024, **146**, 2333–2338.
15 M. T. Nguyen, D. Gusev, A. Dmitrienko, B. M. Gabidullin, D. Spasyuk, M. Pilkington and G. I. Nikonov, *J. Am. Chem. Soc.*, 2020, **142**, 5852–5861.
16 T. Kuwabara, M. Nakada, J. Hamada, J. D. Guo, S. Nagase and M. Saito, *J. Am. Chem. Soc.*, 2016, **138**, 11378–11382.
17 E. C. Neeve, S. J. Geier, I. A. I. Mkhalid, S. A. Westcott and T. B. Marder, *Chem. Rev.*, 2016, **116**, 9091–9161.
18 A. Barthélemy, H. Scherer, H. Weller and I. Krossing, *Chem. Commun.*, 2023, **59**, 1353–1356.
19 H. Braunschweig, R. D. Dewhurst, K. Hammond, J. Mies, K. Radacki and A. Vargas, *Science*, 2012, **336**, 1420–1422.
20 (*a*) A. M. Davis and K. D. McKeegan, *Treatise on Geochemistry*, Elsevier, 2014, pp. 361–395; (*b*) C. Leroy and D. L. Bryce, *Prog. Nucl. Magn. Reson. Spectrosc.*, 2018, **109**, 160–199.
21 G. Wang, J. E. Walley, D. A. Dickie, S. Pan, G. Frenking and R. J. Gilliard, *J. Am. Chem. Soc.*, 2020, **142**, 4560–4564.
22 G. Wang, J. E. Walley, D. A. Dickie, A. Molino, D. J. D. Wilson and R. J. Gilliard, *Angew. Chem.*, 2021, **133**, 9493–9497.
23 M. Arrowsmith, H. Braunschweig, M. A. Celik, T. Dellermann, R. D. Dewhurst, W. C. Ewing, K. Hammond, T. Kramer, I. Krummenacher, J. Mies, K. Radacki and J. K. Schuster, *Nat. Chem.*, 2016, **8**, 638–642.
24 J. T. Boronski, L. R. Thomas-Hargreaves, M. A. Ellwanger, A. E. Crumpton, J. Hicks, D. F. Bekiş, S. Aldridge and M. R. Buchner, *J. Am. Chem. Soc.*, 2023, **145**, 4408–4413.
25 M. R. Buchner, S. Pan, C. Poggel, N. Spang, M. Müller, G. Frenking and J. Sundermeyer, *Organometallics*, 2020, **39**, 3224–3231.
26 M. R. Buchner, L. K. Kreuzer, L. R. Thomas-Hargreaves, M. Müller, S. I. Ivlev, G. Frenking and S. Pan, *Chem. – Eur. J.*, 2024, **30**, e202400966.
27 C. Czernetzki, M. Arrowsmith, L. Endres, I. Krummenacher and H. Braunschweig, *Inorg. Chem.*, 2024, **63**, 2670–2678.
28 G. Wang, L. A. Freeman, D. A. Dickie, R. Mokrai, Z. Benkő and R. J. Gilliard, *Chem. – Eur. J.*, 2019, **25**, 4335–4339.
29 J. T. Boronski, A. E. Crumpton, A. F. Roper and S. Aldridge, *Nat. Chem.*, 2024, **16**, 1295–1300.
30 J. T. Boronski, A. E. Crumpton and S. Aldridge, *J. Am. Chem. Soc.*, 2024, **146**, 35208–35215.
31 J. T. Boronski, A. E. Crumpton, J. J. C. Struijs and S. Aldridge, *J. Am. Chem. Soc.*, 2025, **147**, 10073–10077.
32 M. Dietz, J. T. Boronski, A. M. Swarbrook and S. Aldridge, *Angew. Chem., Int. Ed.*, 2025, **64**, e202503050.
33 C. Helling, D. J. D. Wilson and C. Jones, *J. Am. Chem. Soc.*, 2025, **147**, 16620–16629.
34 (*a*) F. Kraus, S. A. Baer, M. R. Buchner and A. J. Karttunen, *Chem. – Eur. J.*, 2012, **18**, 2131–2142; (*b*) F. Kraus, S. A. Baer, M. Hoelzel and A. J. Karttunen, *Eur. J. Inorg. Chem.*, 2013, **2013**, 4184–4190; (*c*) M. Müller and M. R. Buchner, *Z. Naturforsch., B:J. Chem. Sci.*, 2020, **75**, 483–489; (*d*) M. Müller, A. J. Karttunen and M. R. Buchner, *Chem. Sci.*, 2020, **11**, 5415–5422; (*e*) M. Müller and M. R. Buchner, *Chem. Commun.*, 2019, **55**, 13649–13652.
35 M. R. Buchner, L. R. Thomas-Hargreaves, C. Berthold, D. F. Bekiş and S. I. Ivlev, *Chem. – Eur. J.*, 2023, **29**, e202302495.
36 C. Helling and C. Jones, *Chem. – Eur. J.*, 2023, **29**, e202302222.
37 (*a*) M. Arrowsmith, M. S. Hill, G. Kociok-Köhn, D. J. MacDougall and M. F. Mahon, *Angew. Chem., Int. Ed.*, 2012, **51**, 2098–2100; (*b*) M. Arrowsmith, M. S. Hill, G. Kociok-Köhn, D. J. MacDougall, M. F. Mahon and I. Mallov, *Inorg. Chem.*, 2012, **51**, 13408–13418; (*c*) M. S. Hill, *Inorg. Chem.*, 2013, **109**, 18; (*d*) J. Gottfriedsen and S. Blaurock, *Organometallics*, 2006, **25**, 3784–3786.
38 R. J. Gilliard, M. Y. Abraham, Y. Wang, P. Wei, Y. Xie, B. Quillian, H. F. Schaefer, P. V. R. Schleyer and G. H. Robinson, *J. Am. Chem. Soc.*, 2012, **134**, 9953–9955.
39 (*a*) K. Ruhlandt-Senge, R. A. Bartlett, M. M. Olmstead and P. P. Power, *Inorg. Chem.*, 1993, **32**, 1724–1728; (*b*) R. Fernández and E. Carmona, *Eur. J. Inorg. Chem.*, 2005, **2005**, 3197–3206.
40 M. Müller and M. R. Buchner, *Chem. – Eur. J.*, 2020, **26**, 9915–9922.
41 M. Niemeyer and P. P. Power, *Inorg. Chem.*, 1997, **36**, 4688–4696.
42 (*a*) M. R. Buchner, *Chem. – Eur. J.*, 2019, **25**, 12018–12036; (*b*) M. R. Buchner, *Chem. Commun.*, 2025, **61**, 11146–11157; (*c*) L. A. Freeman, J. E. Walley and R. J. Gilliard, *Nat. Synth.*, 2022, **1**, 439–448; (*d*) D. Parveen, R. K. Yadav and D. K. Roy, *Chem. Commun.*, 2024, **60**, 1663–1673.
43 (*a*) L. R. Thomas-Hargreaves, Y.-Q. Liu, Z.-H. Cui, S. Pan and M. R. Buchner, *J. Comput. Chem.*, 2023, **44**, 397–405; (*b*) H. Brger, C. Forker and J. Goubeau, *Monatsh. Chem.*, 1965, **96**, 597–601; (*c*) J. K. Schuster, D. K. Roy, C. Lenczyk, J. Mies and H. Braunschweig, *Inorg. Chem.*, 2019, **58**, 2652–2658; (*d*) K. G. Pearce, M. S. Hill and M. F. Mahon, *Chem. Commun.*, 2023, **59**, 1453–1456.
44 D. F. Bekiş, L. R. Thomas-Hargreaves, S. I. Ivlev and M. R. Buchner, *Dalton Trans.*, 2024, **53**, 15551–15564.

 

45 D. Naglav, A. Neumann, D. Bläser, C. Wölper, R. Haack, G. Jansen and S. Schulz, *Chem. Commun.*, 2015, **51**, 3889–3891.
46 T. J. Hadlington and T. Szilvási, *Nat. Commun.*, 2022, **13**, 461.
47 (*a*) M. Bayram, D. Naglav, C. Wölper and S. Schulz, *Organometallics*, 2017, **36**, 467–473; (*b*) M. R. Buchner, M. Müller and S. S. Rudel, *Angew. Chem., Int. Ed.*, 2017, **56**, 1130–1134; (*c*) M. R. Buchner, M. Müller, F. Dankert, K. Reuter and C. von Hänisch, *Dalton Trans.*, 2018, **47**, 16393–16397; (*d*) L. R. Thomas-Hargreaves, S. Pan, S. I. Ivlev, G. Frenking and M. R. Buchner, *Inorg. Chem.*, 2022, **61**, 700–705.
48 A. Paparo, C. D. Smith and C. Jones, *Angew. Chem., Int. Ed.*, 2019, **58**, 11459–11463.
49 *Encyclopedia of Inorganic and Bioinorganic Chemistry*, ed. R. A. Scott, Wiley, 2012.
50 (*a*) P. P. Power, *Nature*, 2010, **463**, 171–177; (*b*) P. P. Power, *Chem. Rec.*, 2012, **12**, 238–255; (*c*) N. A. Giffin and J. D. Masuda, *Coord. Chem. Rev.*, 2011, **255**, 1342–1359.
51 (*a*) K. C. Mondal, P. P. Samuel, H. W. Roesky, R. R. Aysin, L. A. Leites, S. Neudeck, J. Lübben, B. Dittrich, N. Holzmann, M. Hermann and G. Frenking, *J. Am. Chem. Soc.*, 2014, **136**, 8919–8922; (*b*) Y. Wang, M. Karni, S. Yao, A. Kaushansky, Y. Apeloig and M. Driess, *J. Am. Chem. Soc.*, 2019, **141**, 12916–12927; (*c*) J. Keuter, A. Hepp, C. Mück-Lichtenfeld and F. Lips, *Angew. Chem., Int. Ed.*, 2019, **58**, 4395–4399; (*d*) M. Y.-S. Wee, S. Quek, C.-S. Wu, M.-D. Su and C.-W. So, *J. Am. Chem. Soc.*, 2024, **146**, 14410–14415; (*e*) S. Du, H. Jia, H. Rong, H. Song, C. Cui and Z. Mo, *Angew. Chem., Int. Ed.*, 2022, **61**, e202115570; (*f*) Y. Xiong, S. Yao, G. Tan, S. Inoue and M. Driess, *J. Am. Chem. Soc.*, 2013, **135**, 5004–5007.
52 (*a*) K. C. Mondal, S. Roy, B. Dittrich, D. M. Andrada, G. Frenking and H. W. Roesky, *Angew. Chem., Int. Ed.*, 2016, **55**, 3158–3161; (*b*) K. C. Mondal, H. W. Roesky, M. C. Schwarzer, G. Frenking, B. Niepötter, H. Wolf, R. Herbst-Irmer and D. Stalke, *Angew. Chem., Int. Ed.*, 2013, **52**, 2963–2967.
53 M. Gimferrer, S. Danés, E. Vos, C. B. Yildiz, I. Corral, A. Jana, P. Salvador and D. M. Andrada, *Chem. Sci.*, 2022, **13**, 6583–6591.
54 S. Pan and G. Frenking, *Chem. Sci.*, 2023, **14**, 379–383.
55 M. Gimferrer, S. Danés, E. Vos, C. B. Yildiz, I. Corral, A. Jana, P. Salvador and D. M. Andrada, *Chem. Sci.*, 2023, **14**, 384–392.
56 T. Arnold, H. Braunschweig, W. C. Ewing, T. Kramer, J. Mies and J. K. Schuster, *Chem. Commun.*, 2015, **51**, 737–740.
57 (*a*) S. P. Green, C. Jones and A. Stasch, *Science*, 2007, **318**, 1754–1757; (*b*) C. Jones, *Nat. Rev. Chem.*, 2017, **1**, 0059; (*c*) S. Krieck, H. Görls, L. Yu, M. Reiher and M. Westerhausen, *J. Am. Chem. Soc.*, 2009, **131**, 2977–2985.
58 P. Pyykkö, *J. Phys. Chem. A*, 2015, **119**, 2326–2337.
59 R. D. Dewhurst, E. C. Neeve, H. Braunschweig and T. B. Marder, *Chem. Commun.*, 2015, **51**, 9594–9607.
60 C. Berthold, J. Maurer, L. Klerner, S. Harder and M. R. Buchner, *Angew. Chem., Int. Ed.*, 2024, **63**, e202408422.
61 C. Berthold, M. H. Lochte and M. R. Buchner, *Chem. – Eur. J.*, 2025, **31**, e202500673.
62 W. J. Haws, *JOM*, 2000, **52**, 35–37.
63 J. T. Boronski, L. P. Griffin, C. Conder, A. E. Crumpton, L. L. Wales and S. Aldridge, *Chem. Sci.*, 2024, **15**, 15377–15384.
64 P. P. Power, *Chem. Rev.*, 1999, **99**, 3463–3504.
65 L. Wang, S. Pan, G. Wang, X. Zeng, M. Zhou and G. Frenking, *Chem. Commun.*, 2022, **58**, 8532–8535.
66 (*a*) J. L. Dutton and D. J. D. Wilson, *Dalton Trans.*, 2018, **47**, 12633–12641; (*b*) L.-J. Cui, X.-B. Liu and Z.-H. Cui, *Inorg. Chem.*, 2025, **64**, 1718–1725.
67 R. Liu, L. Qin, Z. Zhang, L. Zhao, F. Sagan, M. Mitoraj and G. Frenking, *Chem. Sci.*, 2023, **14**, 4872–4887.
68 (*a*) M. K. Sharma, D. Rottschäfer, S. Blomeyer, B. Neumann, H.-G. Stammler, M. van Gastel, A. Hinz and R. S. Ghadwal, *Chem. Commun.*, 2019, **55**, 10408–10411; (*b*) M. K. Sharma, D. Rottschäfer, B. Neumann, H.-G. Stammler, S. Danés, D. M. Andrada, M. van Gastel, A. Hinz and R. S. Ghadwal, *Chem. – Eur. J.*, 2021, **27**, 5803–5809; (*c*) H. Steffenfauseweh, Y. V. Vishnevskiy, B. Neumann, H.-G. Stammler, D. D. Snabilié, B. de Bruin and R. S. Ghadwal, *Angew. Chem., Int. Ed.*, 2025, **64**, e202505142; (*d*) Y.-J. Lin, W.-C. Liu, Y.-H. Liu, G.-H. Lee, S.-Y. Chien and C.-W. Chiu, *Nat. Commun.*, 2022, **13**, 7051.